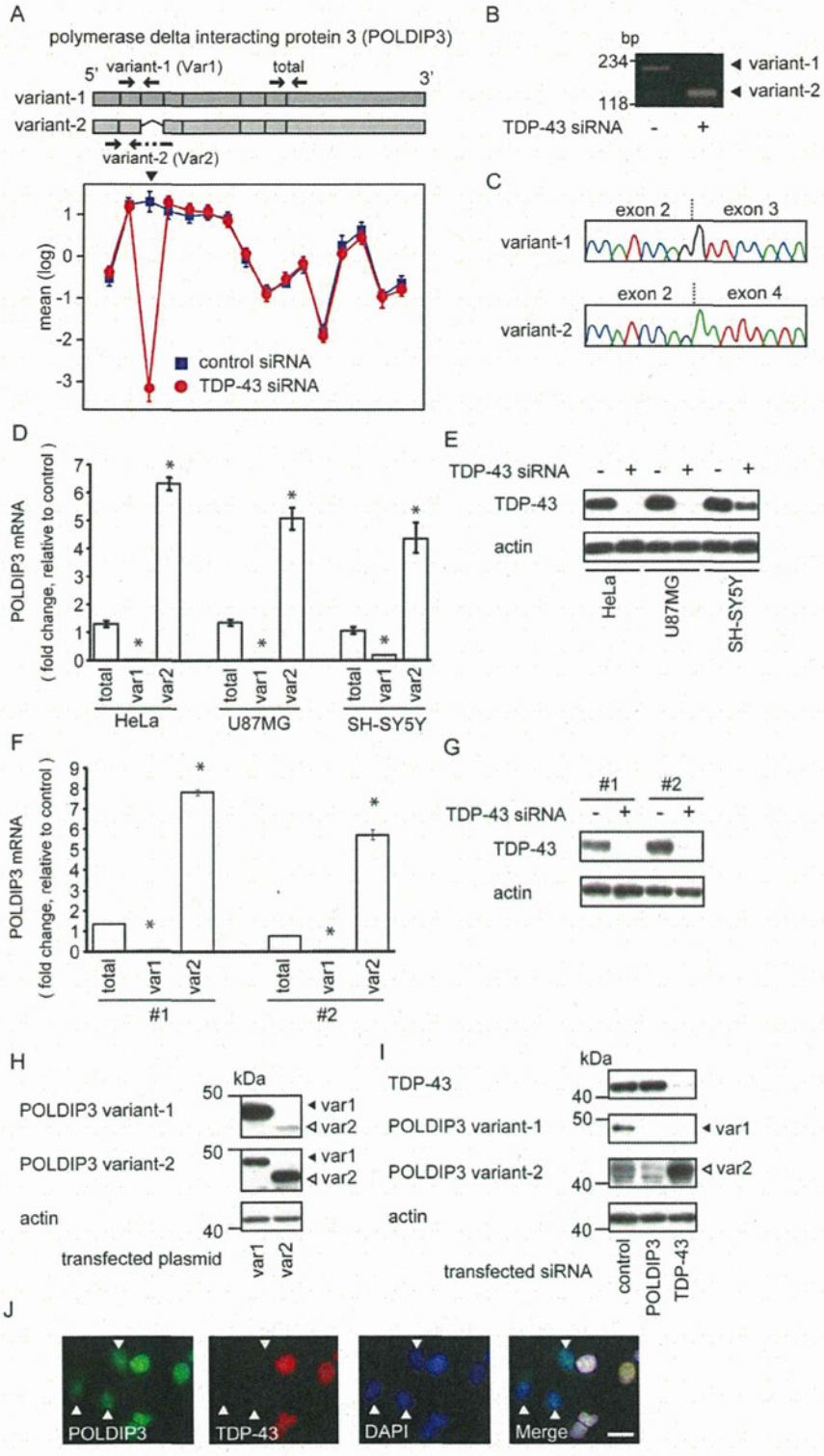

Figure 2. Depletion of TDP-43 mRNA causes aberrant splicing of *POLDIP3* mRNA. (**A**) Alteration of the splicing patterns of *POLDIP3* exon 3. The exon structure of the *POLDIP3* variant-1 (including exon 3) and variant-2 (lacking exon 3) (upper) are shown. Boxes indicate each exon. Arrows indicates the position of primer for amplification of each splicing variant (variant-1 or variant-2) and both *POLDIP3* variants (total). These primers were used in Fig. 2D and F. The gene views show the expression of exons as determined by analyzing the results of the exon array in HeLa cells using Genespring GX. The expression levels are shown on a log2 scale; the error bars show standard errors of means. TDP-43 siRNA, red circle; control siRNA, blue square. Arrowhead shows the probe on *POLDIP3* exon 3. (**B**) The results of an RT-PCR assay with the use of primers spanning *POLDIP3* exon 3 from control or TDP-43 deleted cells (indicate as TDP-43 siRNA +). (**C**) The electropherograms show that variant-1 includes exon 3, whereas variant-2 excludes exon 3. (**D** and **F**) *POLDIP3* mRNA levels in culture cells transfected with TDP-43 siRNA as a fold change relative to those of cells transfected with control siRNA. The amounts of variant-1 (var1), variant-2 (var2), or both (total) *POLDIP3* mRNA were quantified using primers

indicated with arrows in Fig. 2A. *RPLP1* and *RPS18* were used as reference genes. Data represent the mean with standard error from three independent experiments. Asterisk indicates significant difference (*$P<0.01$, Student *t* test). (**D**) Three different cultured cell lines were transfected with TDP-43 siRNA. (**F**) HeLa cells transfected with two additional TDP-43 siRNAs (#1 and #2). (**E** and **G**) Expression of TDP-43 in analyzed cells. TDP-43 was effectively depleted in cells transfected with TDP-43 siRNA. (**H**) Evaluation of anti-POLDIP3 antibodies for each splicing variant of POLDIP3. HEK293T cells were transfected with a POLDIP3 variant-1 or POLDIP3 variant-2 expression vector. POLDIP3 is shown by immunoblotting with the use of the anti-POLDIP3 variant-1 antibody (var1) or anti-POLDIP3 variant-2 antibody (var2). Note that variant-1 antibody reacts predominantly with POLDIP3 variant-1 (upper panel), and variant-2 antibody reacts predominantly with POLDIP3 variant-2 (middle panel). Anti-actin immunoblotting served as a loading control. (**I**) Depletion of TDP-43 results in a decrement of POLDIP3 variant-1 and increment of variant-2. Cell lysates from the HEK293T cells transfected with POLDIP3 or TDP-43 siRNA were subjected to immunoblotting for TDP-43, POLDIP3 variant-1, and POLDIP3 variant-2. Anti-actin immunoblotting served as a loading control. (**J**) Immunohistochemical analysis of POLDIP3 variant-1. HeLa cells were transfected with TDP-43 siRNA, followed by immunostaining with both anti-POLDIP3 variant-1 antibody and anti-TDP-43 antibody. Arrowheads indicate TDP-43-depressed cells. Scale bar, 20 μm.
doi:10.1371/journal.pone.0043120.g002

TDP-43 functions in exon inclusion as well as exon exclusion [19,20]; however, the precise mechanism for regulation of splicing by TDP-43 is unclear. TDP-43 binds to the intronic or noncoding sequences, preferentially (UG)n sequence, and the position of the TDP-43 binding site is associated with exclusion or inclusion of an exon [19,20]. We have shown that only a small number of the genes, which alter their splicing by depletion of TDP-43, are overlapped between HeLa and SH-SY5Y cells. The result indicates that the splicing regulation of TDP-43 is not simply resulted from the nucleotide sequence but also may be regulated by the interaction with other splice factors, including hnRNP A1, A2, and A2/B1 in each cell [10,11].

Although several studies have reported that the pre-mRNA splicing of genes, including *CFTR*, *apoA-II* and *SMN2*, was regulated by TDP-43 in vitro [8,28,29], our results show that depletion of TDP-43 does not affect the splicing for these genes. However, depletion of TDP-43 altered the pre-mRNA splicing in many genes as previously reported [19,20]. In contrast, relatively small numbers of genes were significantly altered in their amount of expression by depletion of TDP-43. Our results indicated that TDP-43 has relatively small effects in the regulation of the amounts of mRNA than the regulation of the splicing in culture cells.

A recent study revealed the alteration of splicing in the frontal cortex with frontotemporal lobar degeneration with TDP-43-positive inclusions (FTLD-TDP), which is another type of TDP-43 proteinopathy [30]. They found an alteration of splicing for *BIM* (Bcl-2 interacting mediator of cell death) but not for *POLDIP3* in brain from FTLD-TDP. The reason why the alteration of splicing for *POLDIP3* is not observed in their analysis might be related to the difference of analysed region, frontal cortex and motor cortex or spinal cord, or the difference of the residual TDP-43 function. Indeed the intracellular and intra central nervous system distribution of TDP-43-positive inclusions are different between FTLD-TDP and ALS [31,32].

POLDIP3 is a substrate for S6K1, which is downstream of mTOR, and enhances the mTOR/S6K1-dependent translation of mRNA, which is associated with cell size [23,25]. Although it has been shown that the POLDIP3 variant-2 locates in the nucleus as well as variant-1 and retains the functional motif, the function of POLDIP3 variant-2 has not been well elucidated [21,25]. Most recently, it has been reported that the POLDIP3 variant-2 enhanced the mTOR/S6K1-dependent translation of mRNA more, and the depletion of TDP-43 increased cell size in HEK293E cells [26]. The results of our cell size assay in non-neuronal cell lines were consistent with this report. However, we have shown that the depletion of TDP-43 decreased cell size in the SH-SY5Y neuronal cell line. The difference for the effect of the depletion of TDP-43 on cell size could be explained by the cell type difference, neuronal or non-neuronal cell line. In addition, by the rescue experiment for cell size, we showed that POLDIP3 variant-2 is less effective than POLDIP3 variant-1 in regard to improving the size of SH-SY5Y cells reduced by the depletion of TDP-43 (Fig. 5E). Thus, the loss of function of TDP-43 may induce decreased function of POLDIP3 due to alteration of *POLDIP3* splicing, which could result in down-regulation of mTOR/S6K1-dependent translation of mRNA in the neuronal cell line. Although loss of TDP-43 function affects the expression and the splicing of various genes, it would be interesting to investigate the contribution of the alteration of *POLDIP3* splicing to the pathogenesis of ALS.

In conclusion, we have shown that the amounts of *POLDIP3* variant-2 mRNA increased in affected tissues with ALS, indicating the loss of function of TDP-43 in ALS. In addition, increasing the amount of *POLDIP3* variant-2 has a potential to be an ideal and sensitive biomarker to represent the dysfunction of TDP-43, since the *POLDIP3* variant-2 is rarely expressed in normal tissues. Thus, the development of the method to detect the amounts of POLDIP3 variant-2 in cerebrospinal fluid would be interesting to diagnosis and evaluate the progression of ALS.

Materials and Methods

Subjects

Details of the patients and controls included in this study are compiled in Table S1. This study was approved by the Institutional Review Board of Niigata University, and written informed consent was obtained from families.

Plasmid constructs

Full-length human TDP-43 complementary DNA (cDNA) and full-length human POLDIP3 cDNA were isolated from the human whole-brain cDNA library (Clontech, Palo Alto, CA, USA) and subcloned into the pcDNA DEST-40 (Invitrogen, Carlsbad, CA, USA) and Vivid colors pcDNA6.2/EmGFP vector (Invitrogen). Human POLDIP3 variant-2 expression plasmid was generated using KOD plus mutagenesis kit (TOYOBO, Osaka, Japan). Mutant TDP-43s (mRRM1, mRRM2, mRRM1/2) expression plasmids were generated with the use of the GeneTailor site-directed mutagenesis system (Invitrogen).

Cell culture and transfection

We cultured HeLa, SH-SY5Y, U87-MG, and HEK293T cells (American Type Culture Collection, Manassas, VA, USA) in Dulbecco modified Eagle medium supplemented with 10% fetal bovine serum at 37°C in 5% CO_2. Plasmid DNAs were transfected into these cells with Lipofectamine 2000 (Invitrogen) according to the manufacturer's instructions. siRNA transfections were performed twice using lipofectamine RNAi MAX (Invitrogen) with 100 pmol control (ID: D-001810-10) or TDP-43-specific (L-012394-00) or POLDIP3-specific (L-019036-01) siRNAs in 6-well plates (Thermo Fisher Scientific, Bremen, Germany). For a

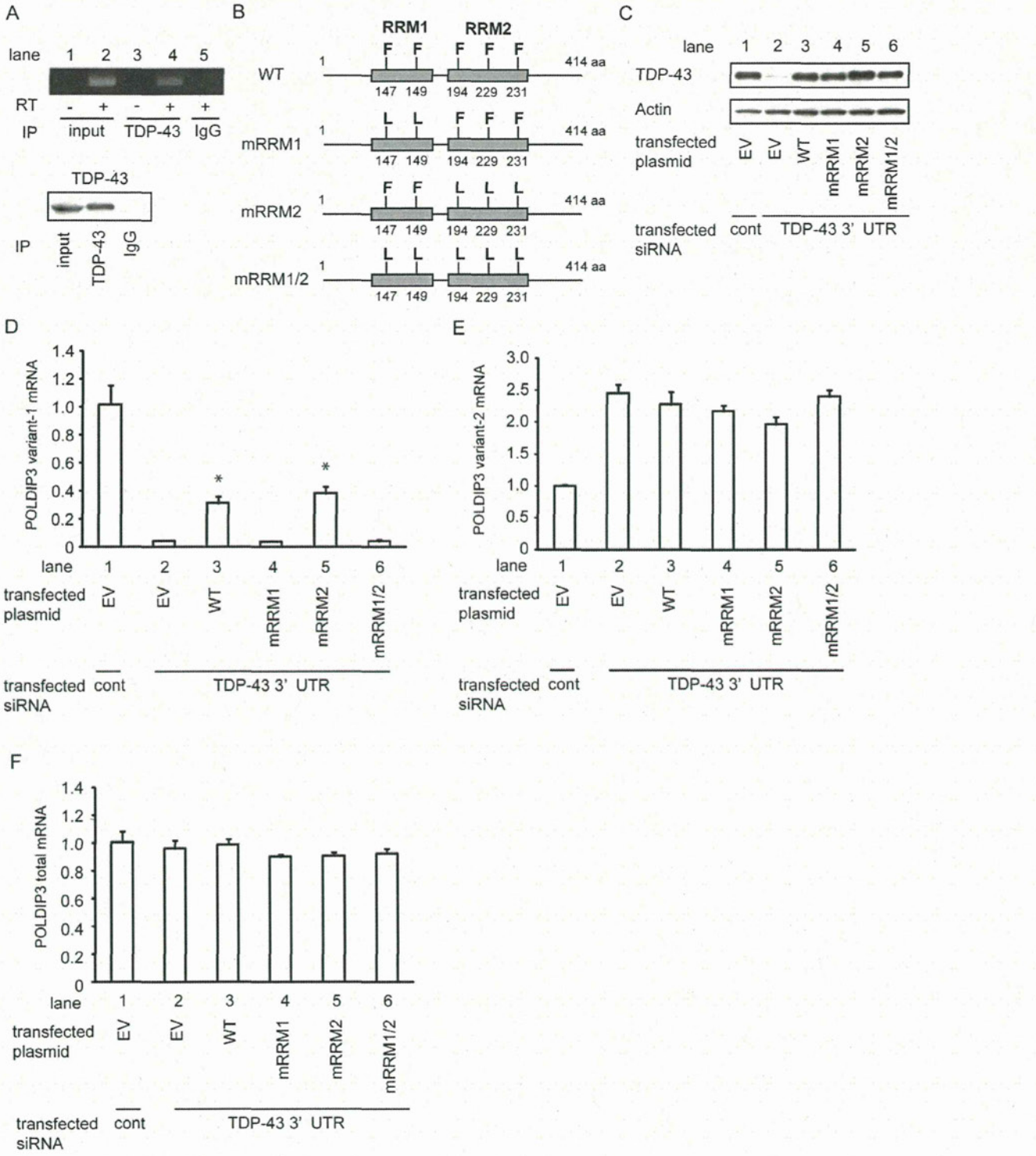

Figure 3. TDP-43 RRM1 domain is necessary for including *POLDIP3* exon 3. (**A**) TDP-43 binds to *POLDIP3* mRNA. Whole cell lysate from HeLa cells was immunoprecipitated with anti-TDP-43 or control rabbit IgG, subjected to the isolation of RNA and RT-PCR analysis using primers located in exon 5 of *POLDIP3*. (**B–F**) Analysis of *POLDIP3* splicing by TDP-43 with mutated in RRM domains. (**B**) Schematic diagram of the constructs for wild-type (WT) and mutated TDP-43 expression plasmid (mRRM1, mRRM2, and mRRM1/2). Phe (F) to Leu (L) alterations were introduced in RRM1, RRM2, or both motifs of the TDP-43. Boxes indicate RRM motif. Numbers indicate the location of substituted amino acids. (**C**) TDP-43 depletion caused by siRNA targeting 3′-UTR of *TDP-43* (TDP-43 3′-UTR siRNA) was rescued by ectopic expression of WT and mutated TDP-43 in HEK293T cells. Mutated TDP-43s were similarly expressed. HEK293T cells were transfected with control (lane 1) or TDP-43 siRNA targeting for 3′-UTR region (lanes 2–6), followed by transfection with empty vector (EV) or various TDP-43 expression plasmids. TDP-43 expression was assessed by probing with anti-TDP-43 antibody. Anti-actin immunoblotting served as a loading control. (**D–F**) *POLDIP3* mRNA levels in culture cells transfected with *TDP-43* 3′-UTR siRNA as a fold change relative to those of cells transfected with control siRNA. The amounts of variant-1 (**D**), variant-2 (**E**) or total *POLDIP3* mRNA (**F**) were quantified

by real-time qRT-PCR using the primers indicated with arrows in Fig. 2A. In this experiment, *RPLP1* and *RPS18* were used as reference genes. Data represent the mean with standard error from three independent experiments. Asterisk indicates significant difference among *TDP-43* 3′-UTR siRNA-transfected cells (*$P<0.01$, Tukey multiple comparison test).
doi:10.1371/journal.pone.0043120.g003

selective depletion for endogenous TDP-43, but not for exogenous TDP-43, we used siRNA targeted to the 3′-UTR of TDP-43 (Hokkaido System Science, Sapporo, Japan). The sequence of TDP-43 siRNA for 3′-UTR as follows: 5′-GAGACUUGGUG-GUGCAUAA-3′.

Western blot analysis

Cells were lysed in RIPA buffer (25 mM Tris-HCl pH 7.6, 150 mM NaCl, 1% NP-40, 1% sodium deoxycholate, 0.1% sodium dodecyl sulfate [SDS]) with protease inhibitor cocktail (1:200, SIGMA, St. Louis, MO, USA) at 4°C. Lysates were centrifuged for 10 minutes at 10,000 *g*, and the resulting supernatants were collected. Protein concentration was determined by BCA protein assay kit (Pierce, Rockford, IL, USA), and equal amounts of protein from cell lysates were analyzed. Lysates were subjected to SDS-polyacrylamide gel electrophoresis and transferred onto polyvinylidene difluoride membranes (Millipore, Bedford, MA, USA). Membranes were incubated with primary antibodies overnight at 4°C, followed by horseradish peroxidase (HRP)-conjugated secondary antibody (1:10,000, SIGMA). TDP-43 was detected with anti-TDP-43 antibody (1:5000, ProteinTech Group, Chicago, IL, USA). POLDIP3 variant-1 was detected with anti-POLDIP3 antibody (1:1000; Cell Signaling, Beverly, MA, USA), and POLDIP3 variant-2 was detected with another anti-POLDIP3 antibody (1:200; Santa Cruz Biotechnology, Santa Cruz, CA, USA). To detect both POLDIP3 variants in Fig. 5C, we used monoclonal rabbit anti-POLDIP3 antibody (1:1000, cell signaling). We detected actin as a loading control using anti-actin antibody (1:1000; Santa Cruz Biotechnology).

Exon array analysis

The Affymetrix GeneChip Whole Transcript Sense Target Labeling Assay was used to generate amplified and biotinylated sense-strand DNA targets (Affymetrix, Santa Clara, CA, USA). Probe was hybridized to Affymetrix 1.0 Human Exon ST arrays according to the manufacturer's instructions (Affymetrix). This array is able to determine the difference at both exon- and gene-level expressions. The arrays were scanned with an Affymetrix Gene Chip scanner 3000 system (Affymetrix). Initial data were processed to CEL file using GeneChip Operating Software (Affymetrix). Analysis of microarray data was performed with Genespring GX ver.11 (Agilent Technologies, Palo Alto, CA, USA). CEL files were imported into the software and their backgrounds underwent Robust Multichip Average and quantile

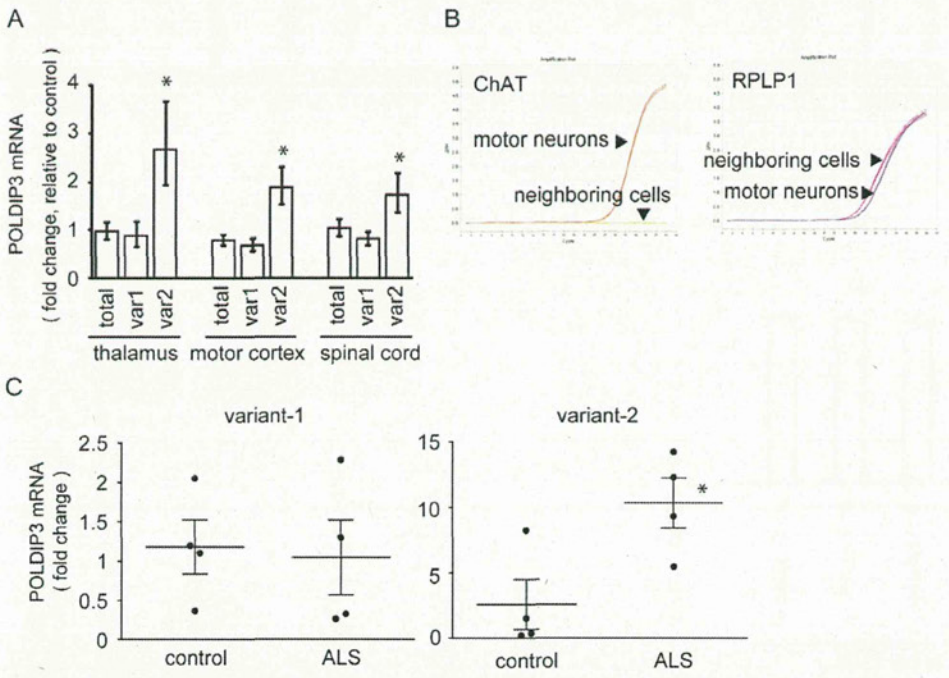

Figure 4. Increased *POLDIP3* variant-2 expression in the CNS with ALS. (**A**) Increased *POLDIP3* variant-2 in CNS with ALS. Total RNA was isolated from the thalamus, motor cortex, and spinal cord of controls ($n=5-7$) and patients with ALS ($n=6-7$) and qRT-PCR analysis was performed using the primers indicated with arrows in Fig. 2A. *POLDIP3* mRNA of total, variant-1, and variant-2 are represented as a fold change relative to controls. In this experiment, *RPLP1* and *RPS18* were used as reference genes. Data represent the mean with standard error. Asterisk indicates significant difference (*$P<0.05$, Student *t* test). (**B**) Purity of the motor neuron enriched material obtained by laser microdissection methods. We isolated 100 motor neurons from L2 in each individual control ($n=4$) or individual with ALS ($n=4$). Real-time qRT-PCR revealed that Tthe expression level of *ChAT* mRNA, a motor neuron marker, was only detected in the motor neuron-enriched material. In contrast, similar expression levels of *RPLP1* mRNA, which was one of the internal controls used in this experiment, were detected in both materials. (**C**) Increased *POLDIP3* variant-2 in ALS motor neurons. *POLDIP3* variant-1 and variant-2 mRNA levels as a fold change relative to those of control are presented by a scatter plot. In this experiment, *RPLP1* and *RPS18* were used as reference genes. Solid line represents the mean with standard error. Asterisk indicates significant difference (*$P<0.05$, Student *t* test).
doi:10.1371/journal.pone.0043120.g004

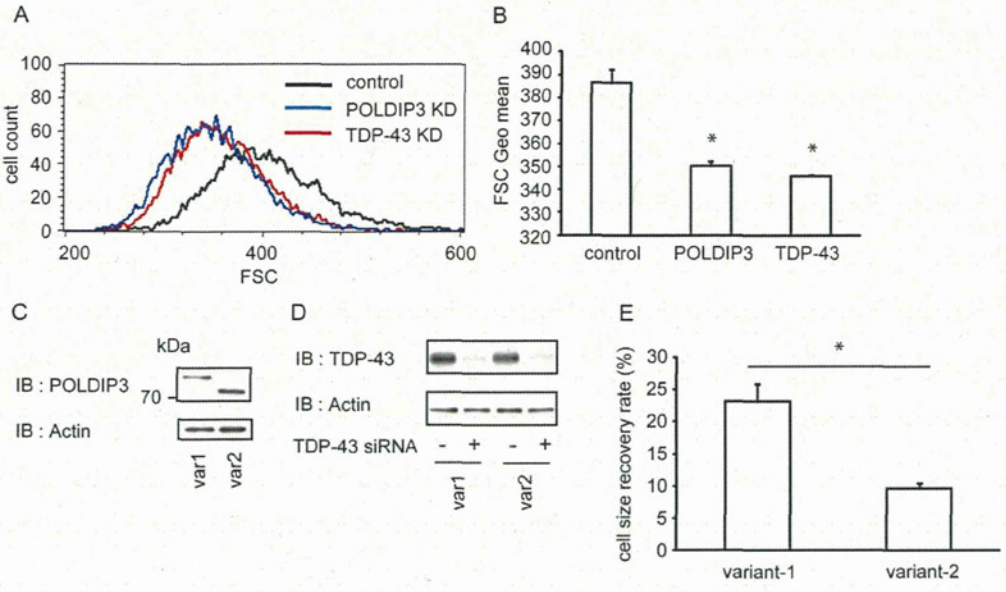

Figure 5. Reduction of TDP-43 expression makes cells smaller. (**A**) A flow cytometer was used to obtain forward scatter (FSC) histograms of SH-SY5Y cells transfected with siRNA targeting POLDIP3 (blue) or TDP-43 (red) or non-targeting control (black). The FSC histogram is one representative transfection from which 10,000 cells were counted. (**B**) Data represent the mean with standard error of forward scatter of the siRNA-transfected cells from three independent experiments. Note that down-regulation of TDP-43 leads to a reduction in cell size as well as POLDIP3 depression. Asterisk indicates significant difference (*$P<0.01$, Tukey multiple comparison test). (**C and D**) Cell lysates from the SHSY5Y cells stably expressed GFP-tagged POLDIP3 variants were subjected to immunoblotting for POLDIP3 (**C**) or TDP-43 (**D**). Anti-actin immunoblotting served as a loading control. (**E**) Recovery rate of the cell size in the TDP-43-depleted SH-SY5Y with or without expression of GFP-tagged POLDIP3 variant. Data represent the mean with standard error from three independent experiments. Note that the cell size recovery rate is significantly increased in the cells expressing POLDIP3 variant-1 compared to in the cells expressing variant-2. Asterisk indicates significant difference (*$P<0.01$, Student *t* test).
doi:10.1371/journal.pone.0043120.g005

normalizations. For our analysis, we have used only the core probe set. Statistical analysis was performed by creating two groups from the individual CEL files, transfection with control siRNA or with TDP-43 siRNA, and then comparing them. From these array data, we calculated the *P* value the splicing index (SI), and fold change. Both a $P<0.05$ and an $|SI|>0.5$ were used as thresholds to identify the aberrant spliced genes, and both a $P<0.05$ and a fold change 2.0 were used for determining differentially expressed genes.

Real-time quantitative RT-PCR analysis

Total RNA was isolated from siRNA transfected cells with the RNeasy plus mini-kit (Qiagen, Valencia, CA, USA). cDNA was synthesized with a high-capacity cDNA reverse transcription kit (Applied Biosystems, Foster City, CA, USA). For autopsied human frozen tissues, mirVana miRNA isolation kit was used to isolate total RNA (Applied Biosystems), followed by synthesis of cDNA using SuperScript® VILOTM cDNA Synthesis Kit (Invitrogen). The RNA quality was assessed by the RNA integrity number (RIN) of the Agilent Bioanalyzer 2100 (Agilent Technologies). RIN score in each sample were described in Table S1. Real-time qRT-PCR was conducted with SYBR Premix Ex Taq on the Thermal Cycler Dice (Takara, Shiga, Japan). Thermal cycler setting was 1) 95°C, 30 sec, 2) 95°C, 15 sec, 3) 60°C, 30 sec and repeat 40 cycles. In each qRT-PCR experiments, Ribosomal protein, large P1 (*RPLP1*) and ribosomal protein S18 (*RPS18*) were used as reference genes, which are determined by geNorm [33]. We designed primer pairs for *POLDIP3* variant-1 and *POLDIP3* variant-2 as follows: POLDIP3 variant-1F: 5′-CAAAACCATC-CAGGTTCCAC-3′, POLDIP3 variant-1R: 5′-AAATTCTGTTTGGCCTGGTG-3′, POLDIP3 variant-2F: 5′-GCTCACCAAAACCATCCAGAA-3′, POLDIP3 variant-2R: 5′- ACTGCTTAGCCCAGCCATGT-3′. The primer design for *MMAB*, *HP1BP3*, *GLS*, *STRA6* and DPM2 as follows: MMAB whole-F: 5′- CAGTGCACATTGCAGGACGTC -3′, MMAB whole-R: 5′- GTACTTGTCGATCCACTGCTC -3′, MMAB variant-F: 5′- CTTAACACTTACCTGTTCCTG -3′, MMAB variant-R: 5′- GAAGCTCTTCGGCAAATGTATG -3′, HP1BP3 whole-F: 5′- GTGAACTCGTCCATCCTAAGG -3′, HP1BP3 whole-R: 5′- CACAGTTCGACGAATCGGCATG -3′, HP1BP3 variant-F: 5′- CTACTTCGAGTGAGGCAGAGC -3′, HP1BP3 variant-R: 5′- GAGTGGAATGAATACTATCAGCTC -3′, GLS whole-F: 5′- GAGTACTGAGCCCTGAAGCAG -3′, GLS whole-R: 5′- CCAGATTTTGCAGGAAGACCAAC -3′, GLS variant-F: 5′- CTTGATCCTCGAAGAGAAGG -3′, GLS variant-R: 5′- CTCATTTGACTCAGGTGACAC -3′, STRA6 whole-F: 5′- GACTACTCCTATGGCAGCTG -3′, STRA6 whole-R: 5′- CACACAGTCAGGCCAGAGCTG -3′, STRA6 variant-F: 5′- CTCCTGAGCTCCCTGTGTTTG -3′, STRA6 variant-R: 5′- GACTAGTCTCAACTCTGTGATC -3′, DPM2 whole-F: 5′- GTCGCCGTTAGCCTGATCATC -3′, DPM2 whole-R: 5′- CAGGAAATACTTGTGGATGAC -3′, DPM2 variant-F: 5′- CAGCATGTCATCCACAAG -3′, DPM2 variant-R: 5′- CTCTTGGTCTTCAGCATCAC -3′. The specificity of each primer was examined using the clones that contained each splicing variant of *POLDIP3*. Predesigned primers were used for *POLDIP3* total, *RPLP1*, and *RPS18* (Takara).

RNA immunoprecipitation (RNA-IP)

RNA-IP was performed using the Magna RIP RNA-Binding Protein Immunoprecipitation Kit following the manufacturer's instructions (Millipore, Billerica, MA, USA). Endogenous TDP-43

protein was immunoprecipitated with anti-TDP-43 antibody (ProteinTech Group) from HeLa cell lysates, and the RNAs isolated from the immunoprecipitated material were subjected to RT-PCR for the *POLDIP3* transcripts. Control rabbit IgG was used as a negative control (Abcam, Cambridge, MA, USA). The primer pairs for *POLDIP3* are as follows; POLDIP3 RNA-IP F: 5′-GCTAAGCAGTTCCAAGCTTTCC-3′, POLDIP3 RNA-IP R: 5′-TGGCAGCTCTTTGGGGGGTT-3′.

Microdissection, total RNA isolation, and qRT-PCR analysis

Frozen sections of spinal cord (10 μm) were stained with HistoGene staining kit (Arcturus Bioscience, Mountain View, CA, USA), followed by microdissection on AS LMD Laser Capture Microdissection System (Leica, Wetzlar, Germany). RNA isolation from microdissected cells was performed using RNAqueous micro kit (Ambion, Austin, TX, USA). cDNA was synthesized with a high-capacity cDNA reverse transcription kit (Applied Biosystems). Before qRT-PCR analysis, cDNA was pre-amplified using the *Taq*Man PreAmp Master Mix (Applied Biosystems) according to the manufacturer's instructions. *Taq*Man gene expression assays were used to determine the expression of *POLDIP3* variant-1 (assay ID: Hs00993978_m1), *POLDIP3* variant-2 (Hs00994038_m1), *RPLP1* (Hs01653088_g1), *RPS18* (Hs02387368_g1), and *ChAT* (Hs00252848_m1) (Applied Biosystems).

Immunohistochemical analysis

Cells were fixed with 4% paraformaldehyde, permeabilized in 0.2% Triton X-100 for 15 minutes and then labeled with primary antibodies. The following antibodies were used: anti-TDP-43 antibody (1:200, Abnova, Taipei, Taiwan), anti-POLDIP3 variant-1 antibody (1:100, Cell Signaling). Images were obtained with an inverted microscope (TE-300NT; Nikon, Tokyo, Japan) and a confocal microscope (CSU-10; Yokogawa Electric, Tokyo, Japan) equipped with a ×100 objective (NA 0.80; Olympus, Tokyo, Japan).

Cell size assay

For determining the cells in G_1 phase, we stained the cells with 7-amino-actinomycin D (7-AAD) according to the manufacturer's instructions (BD Biosciences, San Jose, CA). Briefly, cells were fixed and permeabilized with ice cold 80% methanol and incubated for 1 minute on ice. After washing twice with phosphate-buffered saline, cells were incubated with 7-AAD (SIGMA) for 15 minutes at room temperature in the dark. DNA content was determined by FACSCalibur™ (BD Biosciences) and data were analyzed using CellQuest Pro software (BD Biosciences). The cells with G_0/G_1 phase DNA content were analyzed to determine the cell size.

To further elucidate the functional difference between POLDIP3 variant-1 and POLDIP3 variant-2, we attempted to investigate cell size following treatment with TDP-43 siRNA in SH-SY5Y cells that stably expresses GFP-tagged POLDIP3 variant-1 or variant-2. To estimate the recovery rate of cell size correctly, we used GFP-negative cells in each population as controls. We transfected the cells with TDP-43 or control siRNAs, followed by measuring cell size in each population by FACSCalibur™ (BD Biosciences) and analyzing data by using CellQuest Pro software (BD Biosciences). From the measured value of cell size, we calculated the recovery rate of cell size by comparing the measured value between the cells with or without expression of GFP-tagged POLDIP3 variant. The equation for calculating the recovery rate is as follows:

$$\text{Recovery rate of cellsize } (\%) = (TC/CC - TV/CV)/(TC/CC - 1) \times 100$$

TC = forward scatter of control cells treated with TDP-43 siRNA, CC = forward scatter of control cells treated with control siRNA, TV = forward scatter of cells expressed GFP-tagged POLDIP3 variant treated with TDP-43 siRNA, and CV = forward scatter of cells expressed GFP-tagged POLDIP3 variant treated with control siRNA. The schematic diagram of the cell size rescue experiment is also shown in Fig. S4.

Supporting Information

Figure S1 qRT-PCR analysis for validation of exon array in other 4 genes. (**A**) Exon structure diagram of the main isoform (top) and candidate variant (bottom) for *MMAB, GLS, STRA6, DPM2*. From the exon array result, we selected the candidate splicing variant that was induced by the depletion of TDP-43. The name of each transcript is labeled on the side of the exon structure. The red box indicates the exons that are expected to be altered by TDP-43 depletion. The black bars indicate the position of the primers we used in this experiment. The gene views show the expression of exons as determined by analyzing the results of exon array in HeLa cells using Genespring GX. The expression levels are shown on a log2 scale; the error bars show standard errors of means. TDP-43 siRNA, red circle; control siRNA, blue square. (**B**) qRT-PCR analysis revealed that the splicing alteration of these genes was not validated. *RPLP1* and *RPS18* were used as reference genes. Data represent the mean with standard error from three independent experiments. Asterisk indicates significant difference (*$P<0.01$, Student t test).
(TIF)

Figure S2 Immunohistochemical analysis for TDP-43 in the thalamus. To investigate the presence of TDP-43 pathology in the thalamus from ALS cases used in Figure 4A, TDP-43 immunostaining was performed. Four out of six ALS cases showed (**A**) glial, and (**B–D**) neuronal cytoplasmic TDP-43 immunoreactivity. The label on each figure corresponds to the ID described in Table S1. Scale bar, 20 μm.
(TIF)

Figure S3 Cell size analysis for TDP-43 depressed non-neuronal cells. Data represent the mean with standard error of forward scatter of control or TDP-43 siRNA-transfected cells from three independent experiments. Note that down-regulation of TDP-43 leads to increase cell size in HeLa and HEK293T cells. Asterisk indicates significant difference (*$P<0.01$, Student t test).
(TIF)

Figure S4 The schematic diagram for the cell size rescue experiment by expression of exogenous POLDIP3 variants.
(TIF)

Table S1 Clinical and RNA data for samples in this study. The detailed data for each sample of human material used in this study is shown. Circle indicates the usage for the experients labeled on the top of column. No individual with ALS has a mutation in the *TARDBP* gene. PMI: Post Morten Interval, RIN: RNA Integrity Number.
(XLS)

Acknowledgments

We thank the patients and family members for their participation and M. Tsuchiya, C. Tanda, J. Takasaki, T. Fujita and H. Saito for their technical assistance.

Author Contributions

Conceived and designed the experiments: OO. Performed the experiments: AS TI AM MK TK NW CK. Analyzed the data: AS TI AM TK NW AY. Contributed reagents/materials/analysis tools: MT RK AK MN HT. Wrote the paper: AS HT OO.

References

1. Arai T, Hasegawa M, Akiyama H, Ikeda K, Nonaka T, et al. (2006) TDP-43 is a component of ubiquitin-positive tau-negative inclusions in frontotemporal lobar degeneration and amyotrophic lateral sclerosis. Biochem Biophys Res Commun 351: 602–611.
2. Neumann M, Sampathu DM, Kwong LK, Truax AC, Micsenyi MC, et al. (2006) Ubiquitinated TDP-43 in frontotemporal lobar degeneration and amyotrophic lateral sclerosis. Science 314: 130–133.
3. Tan CF, Eguchi H, Tagawa A, Onodera O, Iwasaki T, et al. (2007) TDP-43 immunoreactivity in neuronal inclusions in familial amyotrophic lateral sclerosis with or without SOD1 gene mutation. Acta Neuropathol 113: 535–542.
4. Kabashi E, Valdmanis PN, Dion P, Spiegelman D, McConkey BJ, et al. (2008) TARDBP mutations in individuals with sporadic and familial amyotrophic lateral sclerosis. Nat Genet 40: 572–574.
5. Sreedharan J, Blair IP, Tripathi VB, Hu X, Vance C, et al. (2008) TDP-43 mutations in familial and sporadic amyotrophic lateral sclerosis. Science 319: 1668–1672.
6. Yokoseki A, Shiga A, Tan CF, Tagawa A, Kaneko H, et al. (2008) TDP-43 mutation in familial amyotrophic lateral sclerosis. Ann Neurol 63: 538–542.
7. Lagier-Tourenne C, Cleveland DW (2009) Rethinking ALS: the FUS about TDP-43. Cell 136: 1001–1004.
8. Buratti E, Baralle FE (2001) Characterization and functional implications of the RNA binding properties of nuclear factor TDP-43, a novel splicing regulator of CFTR exon 9. J Biol Chem 276: 36337–36343.
9. Krecic AM, Swanson MS (1999) hnRNP complexes: composition, structure, and function. Curr Opin Cell Biol 11: 363–371.
10. Buratti E, Brindisi A, Giombi M, Tisminetzky S, Ayala YM, et al. (2005) TDP-43 binds heterogeneous nuclear ribonucleoprotein A/B through its C-terminal tail: an important region for the inhibition of cystic fibrosis transmembrane conductance regulator exon 9 splicing. J Biol Chem 280: 37572–37584.
11. D'Ambrogio A, Buratti E, Stuani C, Guarnaccia C, Romano M, et al. (2009) Functional mapping of the interaction between TDP-43 and hnRNP A2 in vivo. Nucleic Acids Res 37: 4116–4126.
12. Ayala YM, Misteli T, Baralle FE (2008) TDP-43 regulates retinoblastoma protein phosphorylation through the repression of cyclin-dependent kinase 6 expression. Proc Natl Acad Sci U S A 105: 3785–3789.
13. Iguchi Y, Katsuno M, Niwa J, Yamada S, Sone J, et al. (2009) TDP-43 depletion induces neuronal cell damage through dysregulation of Rho family GTPases. J Biol Chem 284: 22059–22066.
14. Sephton CF, Good SK, Atkin S, Dewey CM, Mayer P 3rd, et al. (2010) TDP-43 is a developmentally regulated protein essential for early embryonic development. J Biol Chem 285: 6826–6834.
15. Kraemer BC, Schuck T, Wheeler JM, Robinson LC, Trojanowski JQ, et al. (2010) Loss of murine TDP-43 disrupts motor function and plays an essential role in embryogenesis. Acta Neuropathol 119: 409–419.
16. Kabashi E, Lin L, Tradewell ML, Dion PA, Bercier V, et al. (2010) Gain and loss of function of ALS-related mutations of TARDBP (TDP-43) cause motor deficits in vivo. Hum Mol Genet 19: 671–683.
17. Chiang PM, Ling J, Jeong YH, Price DL, Aja SM, et al. (2010) Deletion of TDP-43 down-regulates Tbc1d1, a gene linked to obesity, and alters body fat metabolism. Proc Natl Acad Sci U S A 107: 16320–16324.
18. Lagier-Tourenne C, Polymenidou M, Cleveland DW (2010) TDP-43 and FUS/TLS: emerging roles in RNA processing and neurodegeneration. Hum Mol Genet 19: R46–64.
19. Tollervey JR, Curk T, Rogelj B, Briese M, Cereda M, et al. (2011) Characterizing the RNA targets and position-dependent splicing regulation by TDP-43. Nat Neurosci 14: 452–458.
20. Polymenidou M, Lagier-Tourenne C, Hutt KR, Huelga SC, Moran J, et al. (2011) Long pre-mRNA depletion and RNA missplicing contribute to neuronal vulnerability from loss of TDP-43. Nat Neurosci 14: 459–468.
21. Smyk A, Szuminska M, Uniewicz KA, Graves LM, Kozlowski P (2006) Human enhancer of rudimentary is a molecular partner of PDIP46/SKAR, a protein interacting with DNA polymerase delta and S6K1 and regulating cell growth. FEBS J 273: 4728–4741.
22. Nishihira Y, Tan CF, Onodera O, Toyoshima Y, Yamada M, et al. (2008) Sporadic amyotrophic lateral sclerosis: two pathological patterns shown by analysis of distribution of TDP-43-immunoreactive neuronal and glial cytoplasmic inclusions. Acta Neuropathol 116: 169–182.
23. Ma XM, Yoon SO, Richardson CJ, Julich K, Blenis J (2008) SKAR links pre-mRNA splicing to mTOR/S6K1-mediated enhanced translation efficiency of spliced mRNAs. Cell 133: 303–313.
24. Fingar DC, Salama S, Tsou C, Harlow E, Blenis J (2002) Mammalian cell size is controlled by mTOR and its downstream targets S6K1 and 4EBP1/eIF4E. Genes Dev 16: 1472–1487.
25. Richardson CJ, Broenstrup M, Fingar DC, Julich K, Ballif BA, et al. (2004) SKAR is a specific target of S6 kinase 1 in cell growth control. Curr Biol 14: 1540–1549.
26. Fiesel FC, Weber SS, Supper J, Zell A, Kahle PJ (2012) TDP-43 regulates global translational yield by splicing of exon junction complex component SKAR. Nucleic Acids Res 40: 2668–2682.
27. Mori F, Tanji K, Miki Y, Kakita A, Takahashi H, et al. (2010) Relationship between Bunina bodies and TDP-43 inclusions in spinal anterior horn in amyotrophic lateral sclerosis. Neuropathol Appl Neurobiol 36: 345–352.
28. Bose JK, Wang IF, Hung L, Tarn WY, Shen CK (2008) TDP-43 overexpression enhances exon 7 inclusion during the survival of motor neuron pre-mRNA splicing. J Biol Chem 283: 28852–28859.
29. Mercado PA, Ayala YM, Romano M, Buratti E, Baralle FE (2005) Depletion of TDP 43 overrides the need for exonic and intronic splicing enhancers in the human apoA-II gene. Nucleic Acids Res 33: 6000–6010.
30. Tollervey JR, Wang Z, Hortobagyi T, Witten JT, Zarnack K, et al. (2011) Analysis of alternative splicing associated with aging and neurodegeneration in the human brain. Genome Res 21: 1572–1582.
31. Mackenzie IR, Baborie A, Pickering-Brown S, Du Plessis D, Jaros E, et al. (2006) Heterogeneity of ubiquitin pathology in frontotemporal lobar degeneration: classification and relation to clinical phenotype. Acta Neuropathol 112: 539–549.
32. Sampathu DM, Neumann M, Kwong LK, Chou TT, Micsenyi M, et al. (2006) Pathological heterogeneity of frontotemporal lobar degeneration with ubiquitin-positive inclusions delineated by ubiquitin immunohistochemistry and novel monoclonal antibodies. Am J Pathol 169: 1343–1352.
33. Vandesompele J, De Preter K, Pattyn F, Poppe B, Van Roy N, et al. (2002) Accurate normalization of real-time quantitative RT-PCR data by geometric averaging of multiple internal control genes. Genome Biol 3: RESEARCH0034.

JNNP Online First, published on September 25, 2012 as 10.1136/jnnp-2012-302272

SHORT REPORT

Japanese amyotrophic lateral sclerosis patients with GGGGCC hexanucleotide repeat expansion in *C9ORF72*

Takuya Konno,[1] Atsushi Shiga,[2] Akira Tsujino,[3] Akihiro Sugai,[1] Taisuke Kato,[1] Kazuaki Kanai,[4] Akio Yokoseki,[1] Hiroto Eguchi,[3] Satoshi Kuwabara,[4] Masatoyo Nishizawa,[1] Hitoshi Takahashi,[2] Osamu Onodera[5]

[1]Department of Neurology, Brain Research Institute, Niigata University, Niigata, Japan
[2]Department of Pathology, Brain Research Institute, Niigata University, Niigata, Japan
[3]First Department of Internal Medicine, Nagasaki University Graduate School of Biomedical Science, Nagasaki, Japan
[4]Department of Neurology, Chiba University School of Medicine, Chiba, Japan
[5]Department of Molecular Neuroscience, Brain Research Institute, Niigata University, Niigata, Japan

Correspondence to
Dr Osamu Onodera, Department of Molecular Neuroscience, Brain Research Institute, Niigata University, 1-757 Asahimachi-dori, Chuo-Ku, Niigata-City, Niigata 951-8585, Japan;
onodera@bri.niigata-u.ac.jp

Received 13 January 2012
Revised 9 July 2012
Accepted 13 July 2012

ABSTRACT

Background A GGGGCC hexanucleotide repeat expansion in *C9ORF72* occurs on a chromosome 9p21 locus that is linked with frontotemporal dementia (FTD) and amyotrophic lateral sclerosis (ALS) in white populations. The diseases resulting from this expansion are referred to as 'c9FTD/ALS'. It has been suggested that c9FTD/ALS arose from a single founder. However, the existence of c9FTD/ALS in non-white populations has not been evaluated.

Results We found two index familial ALS (FALS) patients with c9FTD/ALS in the Japanese population. The frequency of c9FTD/ALS was 3.4% (2/58 cases) in FALS. No patients with sporadic ALS (n=110) or control individuals (n=180) had the expansion.
Neuropathological findings of an autopsy case were indistinguishable from those of white patients. Although the frequency of risk alleles identified in white subjects is low in Japanese, one patient had all 20 risk alleles and the other had all but one. The estimated haplotype indicated that the repeat expansion in these patients was located on the chromosome with the risk haplotype identified in white subjects.

Conclusions *C9ORF72* repeat expansions were present in a Japanese cohort of ALS patients, but they were rare. Intriguingly, Japanese patients appear to carry the same risk haplotype identified in white populations.

INTRODUCTION

A chromosome 9p21 locus has been linked with both familial and sporadic frontotemporal dementia (FTD) and amyotrophic lateral sclerosis (ALS) in white populations.[1–4] It has been identified as a risk haplotype that is represented by a 140 kb block of linkage disequilibrium on chromosome 9p, and rs3849942 allele A is the most commonly associated single nucleotide polymorphism (SNP).[3 5] Recently, a GGGGCC hexanucleotide repeat expansion in the non-coding region of *C9ORF72* was identified in this locus.[6 7] In normal individuals the number of repeats is no more than 23.[6] The number was increased to more than 700 in four patients based on a Southern blot analysis,[6] but the actual threshold and penetrance of expanded repeats of different sizes are still unclear. The diseases resulting from the expansion are now referred to as 'c9FTD/ALS'.[6] The existence of RNA foci in affected cells and a decreased amount of *C9ORF72* mRNA in patients with c9FTD/ALS indicate that the expansion is the causative mutation for c9FTD/ALS.[6–8]

In white populations, c9FTD/ALS is the most frequent cause of familial ALS (FALS) and sporadic ALS (SALS), accounting for 23.5%–47% of FALS incidence and 4.1%–21.0% of SALS incidence.[6–8] Haplotype analysis of affected individuals indicates that c9FTD/ALS arose from a single founder mutation from a common Scandinavian ancestor.[3 5] DeJesus-Hernandez *et al* found that all patients with c9FTD/ALS had rs3849942 allele A, and significantly longer repeats were observed for the haplotype with rs3849942 allele A compared with the haplotype without allele A in control subjects, suggesting that de novo expansion may occur on the risk haplotype.[6] However, it is still controversial whether the expansion occurs on any haplotype or only on the risk haplotype.[7] Investigation of the repeat expansion on different genetic backgrounds may help solve this issue. Here we report two Japanese patients with c9FTD/ALS who appeared to have the same risk haplotype identified in white subjects.

MATERIAL AND METHODS

Mutation screening

Repeat-primed PCR and genotyping PCR for GGGGCC repeats in *C9ORF72* were performed in genomic DNA from 110 patients with SALS, 58 with FALS (unrelated to each other and having at least one first-degree relative diagnosed with ALS), 180 Japanese control subjects and two white patients with c9FTD/ALS as positive control (Coriell Cell Repositories, Camden, New Jersey, USA).[6 7] Fluorescence fragment length analysis of PCR fragments was performed on an ABI 3130xl genetic analyzer (Applied Biosystems, Foster City, California, USA) and with Peak Scanner software v1.0 (Applied Biosystems). This study was approved by the Institutional Review Board of Niigata University, and written informed consent was obtained from all patients or their relatives.

SNP genotyping and haplotype estimation

The risk haplotype consists of 20 SNPs ranged from rs1822723 (centromeric) to rs2477518 (telomeric).[5] The rs3849942 SNP was genotyped using TaqMan

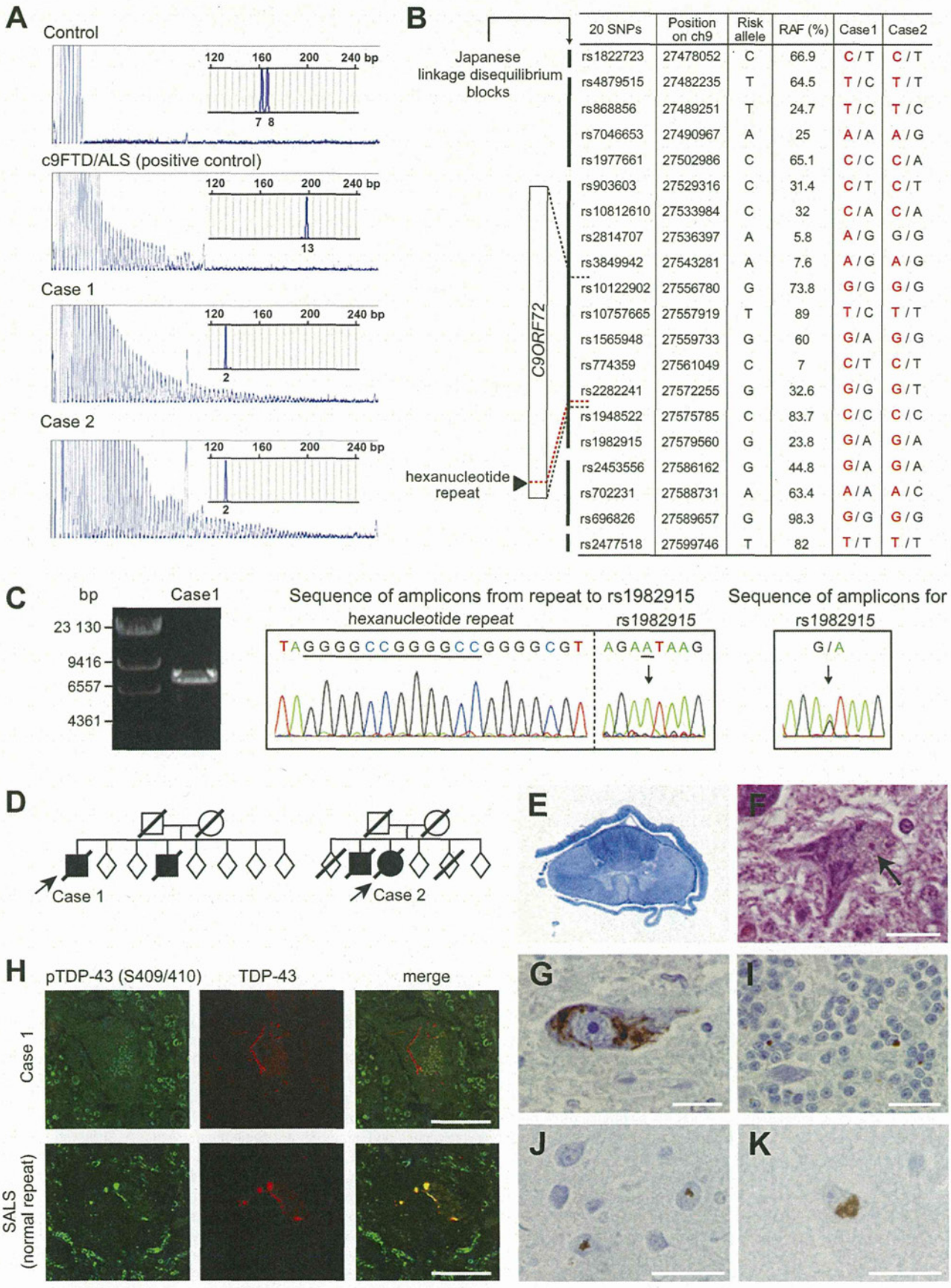

Figure 1 (A) Electropherograms show capillary-based sequence traces of the repeat-primed PCR. The typical sawtooth patterns are observed in the cases carrying the GGGGCC repeat expansion and a positive control.[7] The inset shows fluorescent fragment length analyses of a genotyping PCR fragment containing the GGGGCC repeat in *C9ORF72*. The repeat expansion carriers show one peak due to the presence of an unamplifiable repeat expansion. Numbers under the peaks indicate the number of GGGGCC repeats. (B) Schematic representation of the *C9ORF72* gene and

Konno T, Shiga A, Tsujino A, *et al*. *J Neurol Neurosurg Psychiatry* (2012). doi:10.1136/jnnp-2012-302272

SNP genotyping assays (Applied Biosystems).[6] The other SNPs were analysed by a direct sequencing method. Haplotypes consisting of these SNPs were estimated in 30 Japanese controls using SNPAlyze V.8 (DYNACOM, Chiba, Japan).

Histopathological analysis

For histological analysis, we prepared 4 μm thick, formalin-fixed, paraffin-embedded sections of brain and spinal cord tissue. For immunostaining, we used anti-TDP-43 antibody (ProteinTech Group, Chicago, Illinois, USA), anti-phosphorylated TDP-43 (pTDP-43) antibody (S409/410) (Cosmo bio, Tokyo, Japan) and anti-p62 antibody (BD Transduction Laboratories, San Diego, California, USA) as a primary antibody. Fluorescent images were acquired with an LSM 710 NLO laser-scanning confocal microscope (Zeiss, Jena, Germany).

RESULTS

Genetic studies

We found two index patients with FALS (3.4%) who had the GGGGCC repeat expansion in *C9ORF72* (figure 1A, table 1). Neither patients with SALS nor controls had the repeat expansion. We then investigated whether the patients with FALS shared the risk haplotype for c9FTD/ALS identified in white populations. Although we were unable to obtain DNA samples from their relatives, both patients had the same risk alleles associated with c9FTD/ALS in white subjects; one had all 20 SNPs and the other had all but one, including very rare alleles in Japanese (figure 1B). Based on haplotypes from rs1822723 to rs2477518 in Japanese controls, we estimated that each patient had the risk haplotype (figure 1B). In addition, sequence analyses for amplicons spanning the hexanucleotide repeat to rs1982915 revealed that the normal repeat and the rs1982915 A allele were located on the same chromosome, suggesting that their expanded repeats were located on the risk haplotype (figure 1C). To investigate whether the risk allele was associated with repeat length, we examined the number of repeats in Japanese controls and ALS subjects. Although there were no significant differences in the average number of repeats between groups, the individuals carrying at least one rs3849942 allele A had a significantly longer repeat than those without allele A (table 1).

Case reports

The patients were diagnosed with ALS without dementia. Both patients had a sibling who had also been diagnosed with ALS but their parents had been healthy (figure 1D). There was no family history of dementia such as FTD or other neurological diseases in either family. Case 1 (case 4 in a previous report[9]) noticed hand clumsiness at age 61 years, and progressively developed dysarthria, dysphagia and limb weakness. He died 20 months after onset due to respiratory failure. Case 2 noticed dysarthria at age 63 and gradually developed weakness and muscle atrophy in her tongue and extremities. MRI revealed mild diffuse brain atrophy but the mini-mental state examination score was 29/30. She died 35 months after onset.

Histopathological studies

The brain of the case 1 patient weighed 1340 g and had no apparent abnormalities in its external appearance. Histopathological examination showed degeneration in the spinal anterolateral columns (figure 1E) as well as evidence of neuronal loss and gliosis in the spinal anterior horn, brainstem lower motor neuron nuclei (V, VII and XII) and precentral cortex. Bunina bodies were a feature in the affected lower motor neurons (figure 1F). TDP-43-immunopositive neuronal cytoplasmic inclusions (NCIs) were observed in the brainstem lower motor neuron nuclei, spinal anterior horn (figure 1G) and precentral cortex. In addition, TDP-43-immunopositive oligodendroglial cytoplasmic inclusions (GCIs) were observed in the pyramidal tract. However, pTDP-43-immunopositive NCIs and GCIs were rare. Double-labelling immunofluorescence in the neurons of the cervical anterior horn revealed that TDP-43-immunopositive skein-like inclusions were pTDP-43-immunonegative (figure 1H).

p62-Immunopositive and TDP-43-immunonegative inclusions in the cerebellum and hippocampus have been reported as pathological hallmarks of c9FTD/ALS.[10] In our case, we found p62-immunoreactive NCIs in the cerebellar granule cells (figure 1I) and in the granule cells and pyramidal CA4-CA2 neurons of the hippocampus (figure 1J), which were not recognised by either TDP-43 or pTDP-43 antibodies. p62-Immunopositive inclusions were also observed in the spinal anterior horn and motor cortex (figure 1K), which were recognised by a TDP-43 antibody, but not by a pTDP-43 antibody.

[Continued]

surrounding associated 20 single nucleotide polymorphisms (SNPs).[5] Japanese linkage disequilibrium blocks (indicated by black bars) and risk allele frequencies (RAF) of each SNP in Japanese are presented based on HapMap-JPT (http://www.ncbi.nlm.nih.gov/projects/SNP/). Genotypes of Japanese c9FTD/ALS cases are shown. We estimated the haplotype consisting of these SNPs from control using SNPAlyze V.8 (DYNACOM, Chiba, Japan), and then we estimated the haplotype for each case. Case 1 has the risk haplotype (shown in red) and the most frequent non-risk haplotype (shown in black). Case 2 also has the risk haplotype except rs2814707 (shown in red) and the non-risk haplotype (shown in black). (C) Direct sequence analysis for amplicons spanning the hexanucleotide repeat to rs1982915 from case 1. Approximately 7 kbp amplicons spanning from the hexanucleotide repeat to rs1982915 are shown in the left panel (primer sequences and condition are available on request). Chromatograms for the amplicons are shown in the right panel. Because the PCR cannot amplify the expanded repeat, the amplicons only have the normal repeat. Although both cases have G/A allele for rs1982915 in genotyping, the sequence analysis of the amplicons shows that the products have only the A allele for rs1982915. The same results were obtained for case 2. (D) The pedigree of the cases carrying the repeat expansion. These families had no history of dementia or psychosis. The parents were healthy and without dementia for more than 80 years in case 1 and for more than 65 years in case 2. Arrow, the probands; squares, men; circles, women; solid symbols, affected family members. Sex of the unaffected siblings is obscured to protect privacy. (E) In the thoracic cord, myelin pallor is evident in the anterior and lateral corticospinal tracts (Klüver–Barrera stain). (F) A Bunina body (arrow) is evident in a facial nucleus motor neuron (H&E stain). (G) TDP-43-positive neuronal cytoplasmic inclusions (NCIs) are evident in a cervical anterior horn cell (TDP-43 immunostaining). (H) Double-labelling immunofluorescence staining in the neurons of the cervical anterior horn. In contrast to the colocalisation of TDP-43 and pTDP-43 in sporadic ALS (SALS) without the repeat expansion, case 1 shows that TDP-43-positive skein-like inclusions are negative for pTDP-43. (I–K) Scattered p62-positive NCIs are evident in the cerebellar granule cells (I), hippocampal CA3 neurons (J) and motor cortex (K) (p62 immunostaining). Scale bars, 20 μm. ALS, amyotrophic lateral sclerosis; FTD, frontotemporal dementia.